

Optical chromatography using a photonic crystal fiber with on-chip fluorescence excitation

P. C. Ashok,*¹ R. F. Marchington,¹ P. Mthunzi,^{1,2} T. F. Krauss¹ and K. Dholakia¹

¹*SUPA, School of Physics and Astronomy, University of St. Andrews, North Haugh, St. Andrews, Fife, KY16 9SS, Scotland, UK*

²*Council for Scientific and Industrial Research, National laser Centre, P.O. Box 395, Pretoria, 0001, South Africa*
**pca7@st-andrews.ac.uk*

Abstract: We describe the realization of integrated optical chromatography, in conjunction with on-chip fluorescence excitation, in a monolithically fabricated poly-dimethylsiloxane (PDMS) microfluidic chip. The unique endlessly-single-mode guiding property of the Photonic Crystal Fiber (PCF) facilitates simultaneous on-chip delivery of beams to perform optical sorting in conjunction with fluorescence excitation. We use soft lithography to define the chip and insert the specially capped PCF into it through a predefined fiber channel that is intrinsically aligned with the sorting channel. We compare the performance of the system to a standard ray optics model and use the system to demonstrate both size-driven and refractive index-driven separations of colloids. Finally we demonstrate a new technique of enhanced optofluidic separation of biological particles, by sorting of human kidney embryonic cells (HEK-293), internally tagged with fluorescing microspheres through phagocytosis, from those without microspheres and the separation purity is monitored using fluorescence imaging.

©2010 Optical Society of America

OCIS codes: (170.1530) Cell analysis; (170.2520) Fluorescence microscopy; (170.4520) Optical confinement and manipulation; (350.4855) Optical tweezers or optical manipulation.

References and links

1. T. Imasaka, Y. Kawabata, T. Kaneta, and Y. Ishidzu, "Optical chromatography," *Anal. Chem.* **67**(11), 1763–1765 (1995).
2. S. J. Hart, and A. V. Terray, "Refractive-index-driven separation of colloidal polymer particles using optical chromatography," *Appl. Phys. Lett.* **83**(25), 5316–5318 (2003).
3. S. J. Hart, A. Terray, K. L. Kuhn, J. Arnold, and T. A. Leski, "Optical chromatography of biological particles," *Am. Lab.* **36**, 13 (2004).
4. T. Hatano, T. Kaneta, and T. Imasaka, "Application of optical chromatography to immunoassay," *Anal. Chem.* **69**(14), 2711–2715 (1997).
5. S. J. Hart, A. Terray, J. Arnold, and T. A. Leski, "Preparative optical chromatography with external collection and analysis," *Opt. Express* **16**(23), 18782–18789 (2008).
6. A. Terray, J. D. Taylor, and S. J. Hart, "Cascade optical chromatography for sample fractionation," *Biomicrofluidics* **3**(4), 044106 (2009).
7. S. J. Hart, A. Terray, T. A. Leski, J. Arnold, and R. Stroud, "Discovery of a significant optical chromatographic difference between spores of *Bacillus anthracis* and its close relative, *Bacillus thuringiensis*," *Anal. Chem.* **78**(9), 3221–3225 (2006).
8. K. Dholakia, W. M. Lee, L. Paterson, M. P. MacDonald, R. McDonald, I. Andreev, P. Mthunzi, C. T. A. Brown, R. F. Marchington, and A. C. Riches, "Optical separation of cells on potential energy landscapes: Enhancement with dielectric tagging," *IEEE J. Sel. Top. Quantum Electron.* **13**(6), 1646–1654 (2007).
9. L. Paterson, E. Papagiakoumou, G. Milne, V. Garcés-Chávez, T. Briscoe, W. Sibbett, K. Dholakia, and A. C. Riches, "Passive optical separation within a 'nondiffracting' light beam," *J. Biomed. Opt.* **12**(5), 054017 (2007).
10. D. M. Gherardi, A. E. Carruthers, T. Čížmár, E. M. Wright, and K. Dholakia, "A dual beam photonic crystal fiber trap for microscopic particles," *Appl. Phys. Lett.* **93**(4), 041110 (2008).
11. N. Mortensen, and J. Folkner, "Near-field to far-field transition of photonic crystal fibers: symmetries and interference phenomena," *Opt. Express* **10**(11), 475–481 (2002).
12. J. C. McDonald, D. C. Duffy, J. R. Anderson, D. T. Chiu, H. Wu, O. J. A. Schueller, and G. M. Whitesides, "Fabrication of microfluidic systems in poly(dimethylsiloxane)," *Electrophoresis* **21**(1), 27–40 (2000).
13. T. Kaneta, Y. Ishidzu, N. Mishima, and T. Imasaka, "Theory of optical chromatography," *Anal. Chem.* **69**(14), 2701–2710 (1997).

14. P. C. Ashok, R. F. Marchington, M. Mazilu, T. F. Krauss, and K. Dholakia, "Towards integrated optical chromatography using photonic crystal fiber," K. Dholakia, and C. G. Spalding, eds., (SPIE, 2009), p. 74000R.
15. G. B. Lee, C. Chang, S. Huang, and R. Yang, "The hydrodynamic focusing effect inside rectangular microchannels," *J. Micromech. Microeng.* **16**(5), 1024–1032 (2006).
16. O. Lara, X. D. Tong, M. Zborowski, and J. J. Chalmers, "Enrichment of rare cancer cells through depletion of normal cells using density and flow-through, immunomagnetic cell separation," *Exp. Hematol.* **32**(10), 891–904 (2004).
17. N. Uchida, D. W. Buck, D. P. He, M. J. Reitsma, M. Masek, T. V. Phan, A. S. Tsukamoto, F. H. Gage, and I. L. Weissman, "Direct isolation of human central nervous system stem cells," *Proc. Natl. Acad. Sci. U.S.A.* **97**(26), 14720–14725 (2000).
18. Y. R. Chang, L. Hsu, and S. Chi, "Optical trapping of a spherically symmetric sphere in the ray-optics regime: a model for optical tweezers upon cells," *Appl. Opt.* **45**(16), 3885–3892 (2006).
19. L. Paterson, E. Papagiakoumou, G. Milne, V. Garces-Chavez, S. A. Tatarikova, W. Sibbett, F. J. Gunn-Moore, P. E. Bryant, A. C. Riches, and K. Dholakia, "Light-induced cell separation in a tailored optical landscape," *Appl. Phys. Lett.* **87**(12), 123901 (2005).
20. P. Mthunzi, W. M. Lee, A. C. Riches, C. T. A. Brown, F. J. Gunn-Moore, and K. Dholakia, "Intracellular dielectric tagging for improved optical manipulation of mammalian cells," *IEEE J. Sel. Top. Quantum Electron.* **99**, 1–11 (2009).
21. J. Baumgartl, G. M. Hannappel, D. J. Stevenson, D. Day, M. Gu, and K. Dholakia, "Optical redistribution of microparticles and cells between microwells," *Lab Chip* **9**(10), 1334–1336 (2009).
22. S. I. Simon, and G. W. Schmid-Schönbein, "Biophysical aspects of microsphere engulfment by human neutrophils," *Biophys. J.* **53**(2), 163–173 (1988).
23. R. M. Sanchez-Martin, M. Cuttle, S. Mittoo, and M. Bradley, "Microsphere-based real-time calcium sensing," *Angew. Chem. Int. Ed.* **45**(33), 5472–5474 (2006).
24. V. K. Kodali, W. Roos, J. P. Spatz, and J. E. Curtis, "Cell-assisted assembly of colloidal crystallites," *Soft Matter* **3**(3), 337–348 (2007).

1. Introduction

Optical chromatography is a simple and promising passive sorting technique, which utilizes the interplay between microfluidic drag force and the optical radiation force to achieve spatial separation of microparticles. When a particle in a microfluidic flow encounters a gently focused laser beam propagating coaxially in the opposite direction to the flow, the particle experiences a force against the flow due to the radiation pressure of the laser beam. The particle comes to a rest point where the optical forces are balanced by the Stokes' viscous drag force. The distance of the rest point from the focus of the laser beam is referred to as the retention distance. The retention distance of the particle is dependent upon the size, refractive index and shape of the particle for a fixed laser beam power and fluid flow velocity. Optical chromatography has been applied to the separation of colloidal materials [1,2] and to different species of biological particles [3]. Optical chromatography has also been used to study the *in situ* reaction rates in immunoassays [4]. The field of optical chromatography is maturing with the capability for filtering out, concentrating and collecting a particular species from a mixture of particles for analysis [5].

The major limitations for the application of optical chromatography are the necessity for highly stable fluid flow and the intricate alignment of laser beam required with respect to the chromatography channel [6]. Despite developments in the fluid delivery platforms of optical chromatography systems [5,6], there has been no integrated approach for launching the laser beam into the chromatography chip to date. Coupling of the laser into the fluid channel is typically achieved by free space alignment methods, which requires specialist expertise for every single run of the experiment [7], limiting the application of this technology.

Here, we address the issue of light launching and take a step towards integration by achieving on-chip delivery of laser beam for chromatography using Photonic Crystal Fiber. Choosing the most appropriate waveguide for light delivery and design of the chip are the key factors for achieving this result. A schematic of the chip is shown in Fig. 1, which is fabricated using soft lithography. The major feature of this chip is the use of Large Mode Area Photonic Crystal Fiber (LMA PCF) for the beam delivery into the microfluidic channel. The mode profile of the output beam from LMA PCF satisfies the properties required for efficient spatial separation through optical chromatography, details of which are discussed in the latter part of this article. The endlessly single mode property of the LMA PCF is exploited to launch multiple wavelengths, namely one beam at 1070nm to achieve spatial separation, and another

at 532nm to achieve *in situ* fluorescence excitation. We also address one of the key problems with passive optical sorting, namely the fact that biological cells of similar size are difficult to distinguish [8]. The difference between healthy and diseased cells of the same species is typically much smaller compared to the natural variation in size and refractive index within a given cell population. We have addressed this issue by tagging the target cell population with internalized microspheres through phagocytosis. While demonstrating the concept here with populations that have been allowed to internalize the microspheres versus others that have not, one can envisage that this technique could be used to discriminate between healthy and diseased cells by selective uptake of spheres with specific antibody, thus greatly amplifying their difference in optical properties and making them easily distinguishable [9].

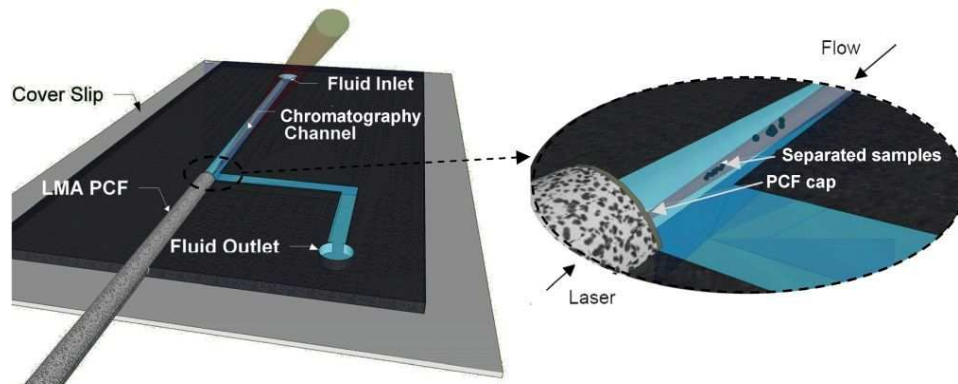


Fig. 1. Design of the chip used for optical chromatography. The pressure driven flow from inlet to outlet was achieved by syringe pumps. The laser beam was delivered to the chip by capped LMA PCF inserted to the predefined fiber channel. The dimensions of the chromatography channel are identical to that of the PCF, being circular in cross section with a diameter of $\sim 240 \mu\text{m}$ and a length of 20mm. [Inset] Closer view of the chromatography channel where a binary sample is spatially separated based on size.

2. Experimental

The success of our approach depends upon the correct choice of optical fiber that achieves a beam with a good TEM_{00} mode profile and a low divergence. In order to get TEM_{00} mode output, we need to use a single mode fiber. The numerical aperture (NA) of standard single mode fiber is comparatively high, (~ 0.13 for fibers at $\lambda = 1070\text{nm}$ operational range) which results in high divergence of the output beam. The use of LMA PCF addresses this issue, as its NA is only ~ 0.055 for a laser of wavelength 1070nm. One of the limitations of a standard single mode fiber based delivery system is that only a narrow bandwidth of wavelengths may typically be delivered through the fiber. However the right choice of endlessly single mode LMA PCF enables us to introduce multiple wavelengths to the chip through the same fiber simultaneously. We use two LMA PCFs of similar performance characteristics for this experiment, LMA - 25 and LMA - 20 PCFs (NKT Photonics). The cladding of this particular fiber consists of a photonic crystal structure with hexagonal symmetry and a solid core, as shown in Fig. 2a. Even though the NA of LMA - 25 is slightly lower (< 0.001) than that of LMA 20, the insertion loss for 532nm laser is higher for LMA - 25 compared to LMA - 20. Therefore, we use LMA 20 for most of the experiments as it presents the best compromise for operation at multiple wavelengths.

The output mode of LMA PCF is hexagonal as shown in Fig. 2b. In the nearfield, the beam first comes to a focus at $150\mu\text{m}$, before slowly diverging [10]. In the far field, the beam profile can be approximated as a hexagonal central lobe with a Gaussian intensity distribution plus six additional satellite lobes, each of which have an intensity two orders of magnitude lower than the peak intensity [11]. Hence the output mode can be approximately described as

a TEM₀₀ Gaussian mode. The large mode area of the fiber also allows easy coupling of the laser source into the fiber.

When immersed into fluids, the holes in the cladding of PCF would naturally fill up due to capillary action, which changes the guiding characteristics of the fiber, resulting in leaky modes and deteriorating the quality of the output beam. To avoid this issue, we devised a capping method to seal the cleaved tip of the fiber using PDMS whilst ensuring that there is no distortion of the output mode profile. The cleaved tip of the LMA PCF is dipped into uncured PDMS for a short time. The controlled dipping procedure ensures minimal suction of PDMS into the holes of PCF due to capillary action. The tip is heated for 8 minutes at 150°C for curing, which forms a perfect seal for the holes in the cladding of LMA PCF.

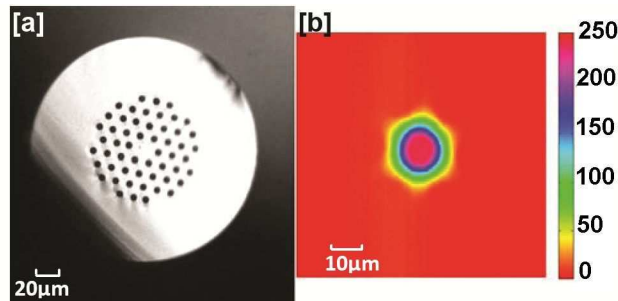


Fig. 2. (a) Cleaved tip of LMA 25 PCF. (b) Intensity map of hexagonal central mode in the output profile of LMA 25 PCF imaged at the tip of the fiber.

The microfluidic chip is fabricated using conventional soft lithographic techniques [12], but with the added novelty of incorporating a section of identical PCF onto the master mold. The fiber, fixed to the master mold defines the fiber channel for the insertion of PCF and the chromatography channel, so that the fiber could directly be inserted to the chromatography channel as shown in Fig. 1. Since we use identical PCF for defining the fiber channel in the mold and for light launching in the experiment, the size of the fiber alignment channel is perfectly matched for fiber insertion, ensuring that the chip is leak-proof. Since the same fiber defines both the fiber channel and fluidic channel, the perfect collinear alignment of the fiber with respect to the fluidic channel is ensured, requiring no further manual adjustments once the fiber is inserted into the chip as shown in Fig. 3.

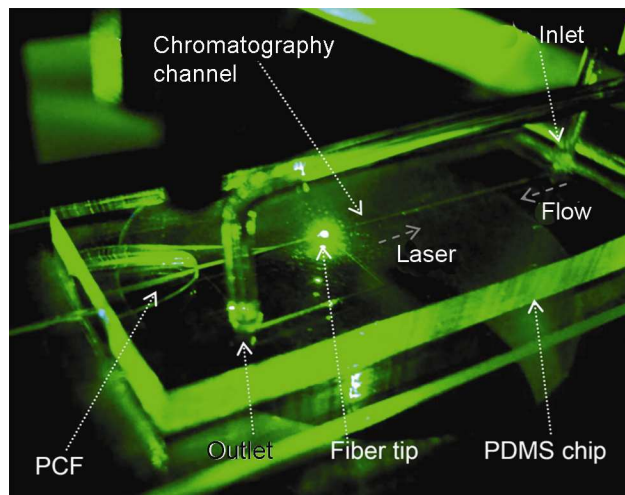


Fig. 3. Integrated optical chromatography chip. PCF is inserted into the chip through a fiber channel and used to simultaneously launch lasers operating at $\lambda = 1070\text{nm}$ and $\lambda = 532\text{nm}$ for spatial separation and fluorescence excitation respectively.

In order to create the master mold, the fiber channel and the fluidic channel are defined by fixing LMA PCF onto the silicon substrate with a thin SU8 layer of thickness 5 μ m. The fluid outlet channel is then defined in thicker SU8 of height 200 μ m. A tapered entrance on the fiber insertion port is defined for easy insertion of the fiber, using UV curable glue (Norland Optical Adhesive 60). A detailed description on the fabrication steps for the mold is given in the appendix. Chips are then molded in PDMS, fluid inlets and outlets punched, and plasma bonded to a glass slide. Once the chip is ready, the LMA PCF used for experiment is directly inserted into the chip through the predefined fiber channel. The fiber channel is leak proof due to the flexibility of PDMS. Since the tip of the fiber is capped, the fiber tip could directly be inserted to the fluidic channel as shown in Fig. 1, which ensures that there would not be any aberration for the beam inside the fluidic chip or the need for index matching fluid.

The optical setup consists of components for coupling the laser into the LMA PCF. In the existing free space optical chromatography designs it is necessary to perform the alignment procedures at each run of the experiment, which requires a specialist. In contrast to that, in our design, once the beam is coupled to the fiber, no further optical alignment is required for different runs of experiments with different chips. It is possible to plug-in the PCF to different PDMS chips, which would be self-aligned to the chromatography channel due to the design of the chip. Coupling of light to the chip through a flexible waveguide (PCF) adds mobility to the chip, which makes it possible to combine the chromatography chip with existing imaging and spectroscopic devices to increase its functionality, allowing the chip to be freely translated to take images or signals from different locations within the chip.

We use a fiber laser operating at wavelength $\lambda = 1070\text{nm}$ (IPG Photonics) and use a fiber coupler (Elliot Scientific) with an $f = 50\text{mm}$ lens to couple the laser into the LMA PCF. The coupling efficiency of the LMA PCF at 1070nm is $>65\%$. Typically, a power of 500mW to 1W is used for spatial separation at the output of PCF. It is possible to further improve the technology to miniaturize the coupling optics by choosing proper pigtailed laser and couplers for launching light to PCF, thereby avoiding the need for bulk optics in the system that would help to make the device completely portable and compact for field applications.

In order to perform on-chip fluorescence, a frequency doubled Nd:YAG laser (Photonics Innovation Centre, University of St Andrews) of $\lambda = 532\text{nm}$ is coupled into LMA PCF by combining the 532nm laser beam with the 1070nm laser beam using a beam splitter. For shorter wavelengths, attenuation is high for LMA PCFs, hence the insertion efficiency for 532nm laser is $<1\%$ for LMA PCF for a length of one meter. In our experiments we use a coupled power of $\sim 40\mu\text{W}$ for fluorescence excitation.

For imaging, a custom made microscope in transmission mode with an infinity corrected long working distance 20X magnification objective (Mitutoyo) is used. A digital CCD camera (The Imaging Source) imaged the position of the particles during experiments.

Stable laminar flow in the microfluidic chip is achieved by pressure driven flow using two syringe pumps (Harvard apparatus pico 11 plus) connected to inlet and outlet for push and pull. Glass syringes of 10 μ l (Gastight, Hamilton) are used in the syringe pump to achieve the desired flow speed in the microfluidic channel. In order to fill the chip and tubing with buffer solution a peristaltic pump (Ismatec Ecoline) is used. Rigid polymer tubing (Upchurch scientific, Tub Radel R, ID- 0.25mm, OD-1.5mm) is used to create the necessary fluid network. In order to achieve greater stability of flow, a T-junction tap (Upchurch Scientific) is used to isolate the inlet and outlet ports from the peristaltic pump during the experiment. The sample fluid is injected into the inlet using a sample injector (6 port injection valve, Upchurch Scientific) without disturbing the flow.

The details of the protocols used for phototransfection and phagocytosis of cells are described in the appendix.

3. Results and discussions

3.1 Calibration of the system

The chromatography system is calibrated using dielectric spheres of silica and polymer (Duke Scientific, polysciences) of sizes 2 μm , 3 μm and 4 μm . Considering a ray optics approximation in order to calculate the radiation force for a sphere of radius a , refractive index n_2 , suspended in a medium of refractive index n_1 , the retention distance can be expressed as [13],

$$z(a, n_2) = \frac{(n_1 \pi \omega_0^2)}{\lambda} \sqrt{\frac{n_1 P Q^* a}{3 \pi \eta v c \omega_0^2} - 1} \quad (1)$$

where λ is the wavelength, P is the power of the laser, ω_0 is the beam waist, η is the viscosity of the water, Q^* is the dimensionless parameter obtained by integrating the term which represents the conversion efficiency of optical radiation pressure arising due to reflection and refraction under ray optics approximation, c is the speed of light and v is the average velocity of microfluidic flow in the microfluidic channel [13]. Using the ray optics model for calculating the retention distance has been validated previously by comparing it with a more rigorous model based on the Maxwell stress tensor implemented using a finite element method [14]. We hence adopt the ray optics model here to calculate the retention distance for comparison with the experimental values.

For the calibration, a 1070nm fiber laser is coupled to the PCF and each type of particle was separately injected into the chromatography device and the retention distance recorded as a function of laser power and average flow speed. In all of the experiments mentioned below, approximately 200 particles are injected to the chromatography channel for one measurement. Figure 4 shows the optical power versus the retention distance for polystyrene and silica microspheres, and Fig. 5 shows the average flow speed versus the retention distance graph. All the measurements of retention distance are performed with ~ 10 particles held at the retention distance in order to eliminate concentration-dependent effects.

At the retention distance corresponding to a particular species, the collected particles tend to move due to the dynamic interaction of the particle with each other. For a higher number of particles held at the retention distance (>30), the dynamic interaction creates instability for the concentrated species and the retention distance of the species fluctuates beyond the resolution required for spatial separation of different species ($>400\mu\text{m}$) as mentioned later in this section. The maximum spread of a single species with the above specified concentration, 3 minutes after injecting the sample into the chip, is measured to be $\sim 100\mu\text{m}$, compared to channel length of $1500\mu\text{m}$ over which we are able to perform spatial separation. We therefore assign an error bar of $100\mu\text{m}$ to the data shown in Figs. 5 and 6.

The fluctuation in the mean distance over time and over multiple run is estimated to be $<50\mu\text{m}$, which is less than the spread of multiple trapped particles. The spread is due to the rescattering of the beam due to the large number of particles. The standard deviation in the size of particles and the parabolic flow profile of the fluid in the flow channel [15] also contributes to this spread. The theoretical calculation of retention distance is performed based on Eq. (1) [13] and the beam waist was assumed to be the beam width at the focal spot of the output of PCF. The experimental data has good agreement with the theoretically calculated data, even though we assumed a Gaussian beam output profile for the PCF, which is clearly only an approximation (Fig. 2). Overall, the calibration data shows that a PCF-based light delivery system can give similar performance characteristics to a free space light delivery system in optical chromatography [5,7].

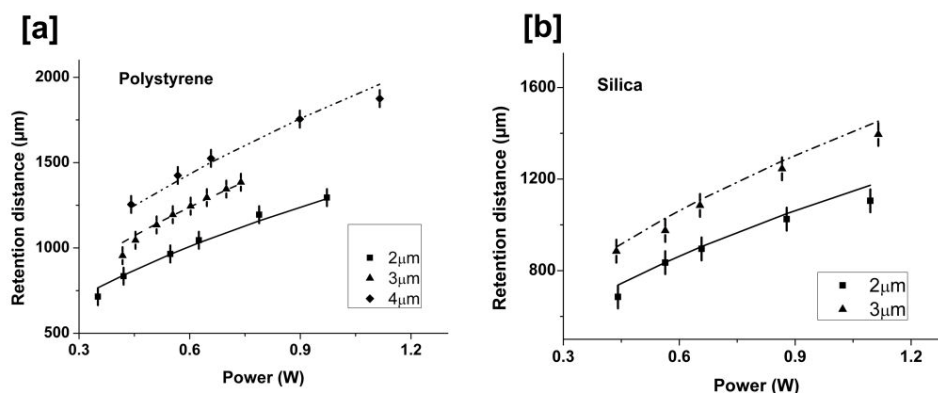


Fig. 4. (a) Retention distance as a function of power for three sizes of polystyrene spheres (Refractive index = 1.59). (b) Retention distance as a function of power for two sizes of silica spheres (Refractive index = 1.43). The dots shows the experimental values of retention distance and the lines show the corresponding values obtained by theoretical calculation based on ray optics model [13]. The error bars show the maximum spread of a single species when ~ 10 particles were held at the retention distance.

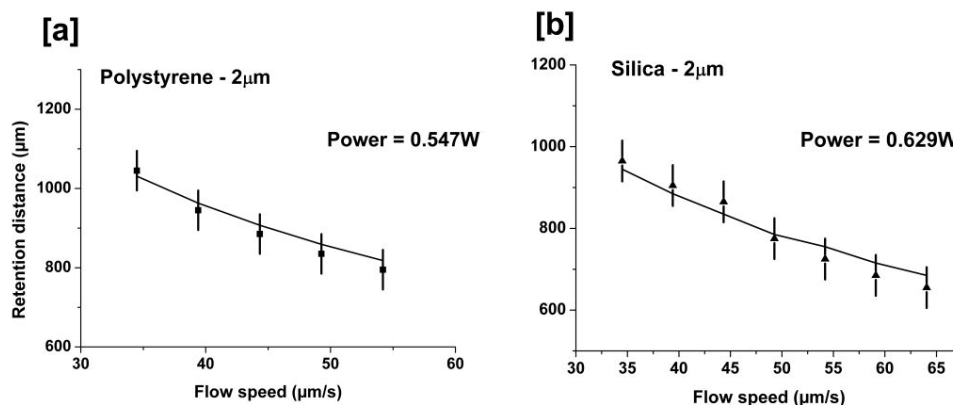


Fig. 5. (a) Retention distance as a function of average flow speed for $2\mu\text{m}$ polystyrene spheres (Refractive index = 1.59). (b) Retention distance as a function of average flow speed for $2\mu\text{m}$ silica spheres (Refractive index = 1.43). The dots show the experimental values of retention distance and the lines show the corresponding values obtained by theoretical calculation based on ray optics model [13]. The error bars show the maximum spread of a single species when ~ 10 particles were held at the retention distance.

The particle separation capability of the system is tested by implementing refractive index driven and size driven separation of binary mixtures of colloids. A binary mixture of $2\mu\text{m}$ and $4\mu\text{m}$ polystyrene particles is spatially separated by a distance of $420\mu\text{m}$ at 520mW power and $34.9\mu\text{m/s}$ average flow speed as shown in Fig. 6a. A binary mixture of $3\mu\text{m}$ polystyrene and silica particle are separated by a distance of $360\mu\text{m}$ at laser power of 1.01W and $39.4\mu\text{m/s}$ average flow speed as shown in Fig. 6b. The separation of species is more than the theoretically calculated value in this case, which might be due to aggregation of polystyrene particles at the equilibrium region.

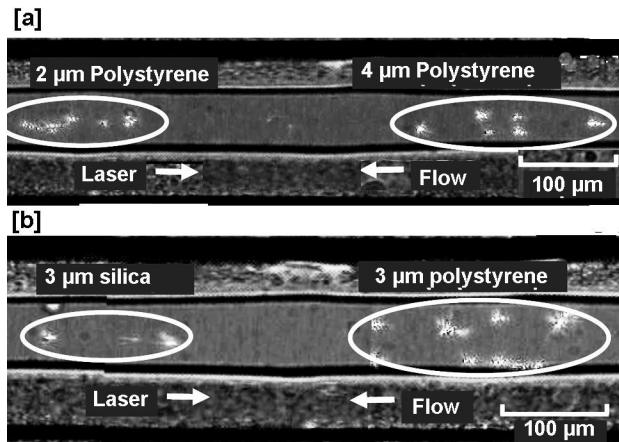


Fig. 6. (a) Size driven separation of binary mixture of polystyrene particles containing spheres of sizes 4µm and 2 µm. (b) Refractive index driven separation of binary mixture of polystyrene particles and silica particles of size 3µm.

3.2 On-Chip fluorescence excitation

As LMA PCF is, in principle, endlessly single mode, it is possible to use it for multiple wavelength delivery on-chip. To demonstrate this potential, a 532nm laser is coupled to the LMA 20 PCF along with the 1070nm chromatography laser, in order to perform on-chip fluorescence excitation. This affords the additional capability of the optical chromatographic system to perform *in situ* monitoring of spatially separated samples provided the sample is fluorescently tagged. Polystyrene beads with red fluorescent dye are used in the system and we demonstrate the possibility to concentrate a sample and analyze it *in situ* with fluorescence imaging. Here, the fluorescence signal is collected on camera, but it could equally have been collected by a spectrometer for fluorescence spectroscopy. HEK cells, photo-transfected with DsRed protein, were retained in the chromatography setup and imaged using on-chip fluorescence excitation as shown in Fig. 7.

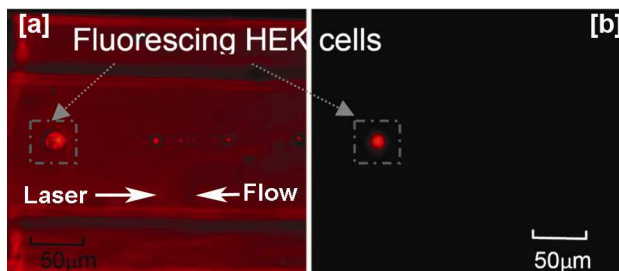


Fig. 7. HEK cells transfected with DsRed protein retained at optical chromatography chip. (a) image with bright field illumination and on-chip fluorescence excitation. (b) Image with on-chip fluorescence excitation.

3.3 Verification of the purity of spatially separated samples

In situ analysis of purity of sample is achieved by spatially separating a binary mixture of colloids of 2µm and 4µm polystyrene out of which 2µm polystyrene beads contained red fluorescent dye. The binary mixture is separated and we observed the number of particles at respective retention distances temporally. The purity of spatially separated sample, observed over 2 minutes, is plotted in Fig. 8. It is clear from Fig. 8 that the 4µm species is comparatively more contaminated with 2µm particles compared to the 2µm species. This shows that the major reason for impurity during spatial separation is aggregation of the

particles in the sample, which increases their effective optical response. The radiation pressure experienced by an aggregated cluster of particles is higher than that of a single particle and hence the retention distance increases for such aggregated clusters of particles, resulting in a higher level of impurity in the sample at a larger retention distance. Multiple runs of the same experiment were performed which gave similar results. Due to different number of particles retained at each run it is not possible to show the data of every run in Fig. 8. A similar experiment is performed with silica beads that show a 100% purity of the spatially separated sample; silica beads, in contrast to polystyrene beads, adhere much more weakly to one another, hence there is a much lower chance of aggregation.

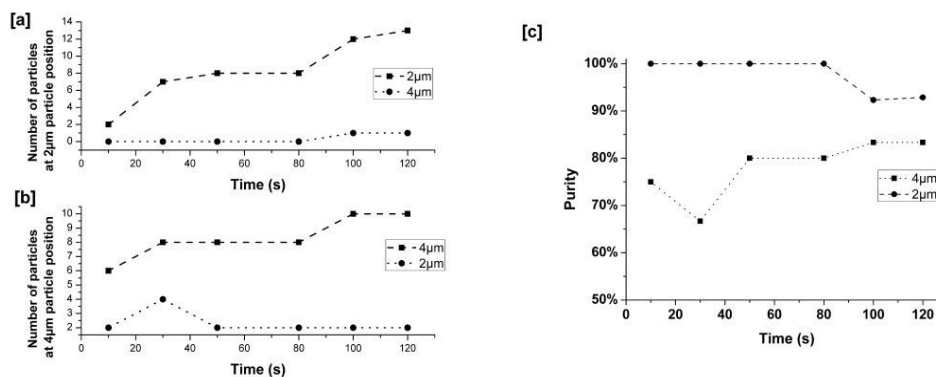


Fig. 8. (a, b) The purity of spatially separated sample observed over 2 minutes for a binary sample of 2µm (red fluorescing) and 4 µm polystyrene microspheres at the (a) 2µm retention location and (b) the 4µm retention location. (c) Purity of the separated sample expressed as a percentage of the total retained particles.

3.4 Separation of mammalian cells incubated with polystyrene beads

In clinical oncology and biomedical research, the ability to rapidly and accurately perform the enrichment and isolation of both rare and not so rare populations of cancerous or stem cells from large mixtures of contaminating cells is highly desirable [16,17]. Passive cell sorting using optical means and at the microfluidic scale is highly attractive. However, in most instances the refractive index of mammalian cells is very close to that of the cell culture medium and/or buffer making them difficult to optically manipulate [18]. It is possible to overcome this hurdle by enhancing the dielectric contrast between different cell types by selectively attaching dielectric spheres [8,9,19]. Recently, we have also reported a new technique for tagging cells without the use of expensive bonding reagents that require careful cell surface chemistry [20,21]. The technique is referred to as phagocytosis or endocytosis and is based on a process whereby foreign particles are naturally internalized by mammalian cells [22]. It is possible to use cells with phagocytosed functionalized microparticles for various intracellular studies, such as calcium signaling detection [23] and cytoskeletal measurements [24].

Here, we demonstrate integrated optical chromatography as an effective optofluidic sorting method to achieve efficient sorting and concentration of cells that contain microspheres, and separate these cells from those that do not contain microspheres, in a species where microspheres were internalized through phagocytosis. Depending on the stage of the cell division cycle during co-incubation with the 2µm polymer spheres, cells engulf different numbers of microspheres, and thus may range from 1 – 5 spheres per cell. HEK-293 cells, incubated with 2µm red fluorescing polystyrene bead are introduced to our optical chromatographic system and spatial separation of the sample is conducted. As shown in Fig. 9, the cells with and without microspheres were separated by a distance of ~650µm at 450mW of laser power for an average flow speed of 26.7µm/s. On-chip fluorescent excitation of the sample with 40µW of 532nm laser, launched through LMA PCF allows *in situ* monitoring of

the purity of spatially separated sample. Observation by fluorescence imaging proves that the spatially separated sample is 100% pure.

The technique of phagocytosis of cells is a simple method to enhance dielectric contrast of cells for active sorting. It is also possible to selectively attach antibody coated beads specific cell types and the responding cell type could then be separated from a mixture using optical chromatography. Hence optical chromatography is shown to be a very effective method to sort cell types in which microspheres have been internalized or selectively attached to in order to enhance the cell's effective refractive index.

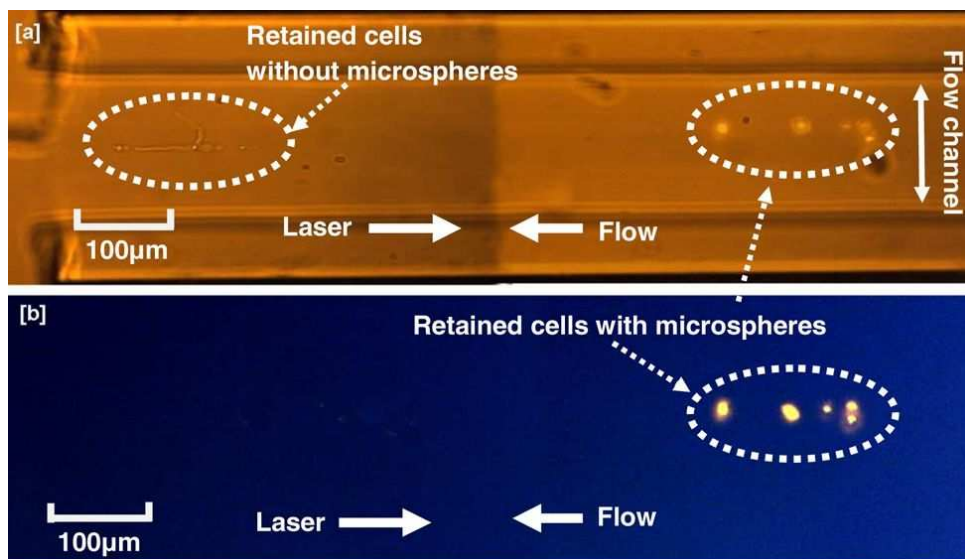


Fig. 9. Separation of HEK cells incubated with red fluorescing polystyrene microspheres. (a) with bright field illumination and fluorescent illumination (b) without bright field illumination and with fluorescent excitation.

4. Conclusion

A novel optical chromatography chip, with integrated launching optics using PCF is successfully implemented and the capability of the system to separate different species of colloidal particles is demonstrated. Since the resultant retention distance is in good agreement with theory, it can be concluded that the resolution of the system is on par with the conventional optical chromatography approaches in which free-space optics are used to couple light into the microfluidic channel. The special characteristics of LMA PCF allow us to launch multiple wavelengths through the fiber to achieve multi-modality by combining optical chromatography with on-chip fluorescence excitation, allowing *in situ* monitoring of the sample during spatial separation. The retention and concentration of HEK cells is achieved in order to demonstrate the capability of the system to sort biological particles. Integrated optical chromatography is shown to be an effective optofluidic sorting method to achieve active sorting of cells internalized with microspheres through phagocytosis, highlighting the flexibility of optical chromatography to be used as both an active and passive sorting technique. The approach based on PCF makes optical chromatography an effective tool to be used with PDMS or indeed other common microfluidic chip materials, and removes the need for free space optical alignment.

Appendix

Steps for the fabrication of the microfluidic chip mold for soft lithography

The mold for the optical chromatography chip is fabricated on a silicon substrate as shown in Fig. 10. A 5 μm layer SU8 is spun on to the silicon substrate and a piece of LMA PCF is placed on the substrate before baking the SU8 layer. The substrate with fiber placed on top, is baked and exposed under UV to cure the SU8 layer so that the 5 μm SU8 layer acts an adhesive to fix the fiber onto the substrate. Further, a 200 μm layer of SU8 is spun on top of the substrate in which the fluid outlet channel is defined using photo-lithography. After completing the development procedures for SU8, a drop of UV curable adhesive is placed at that end of the fiber and cured under UV, producing a taper at the entrance of the channel for easy insertion of the fiber into the chip during experiments. This mold is then used in a standard soft lithography procedure to fabricate the PDMS chip.

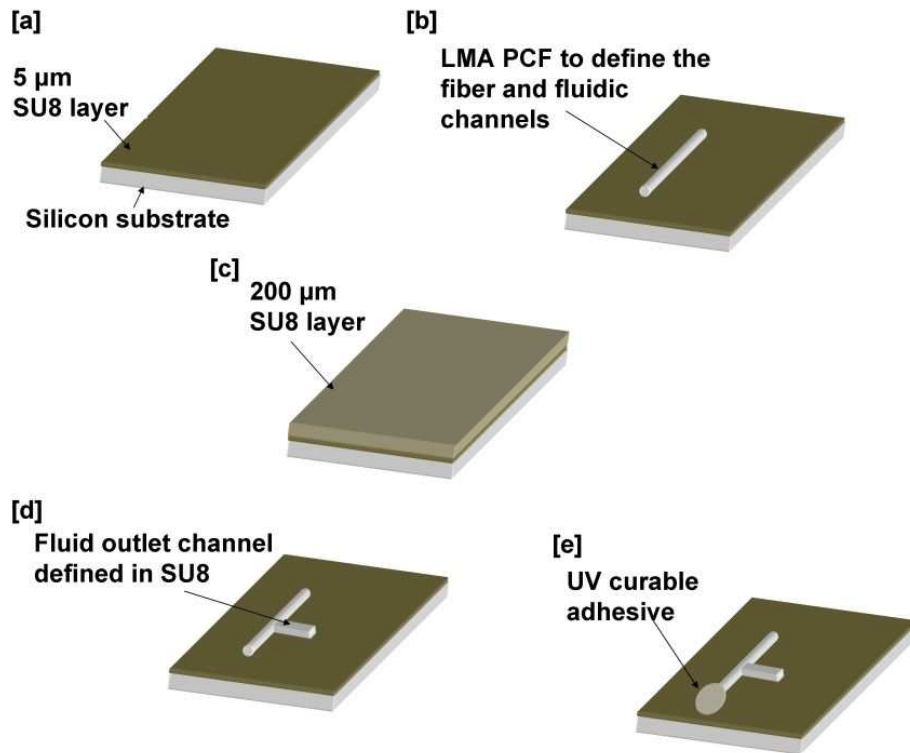


Fig. 10. Different steps in the fabrication of mold (Image not scaled to proportions). (a) A 5 μm SU8 layer spun over a silicon substrate. (b) LMA PCF is placed over the uncured layer of SU8. This composite layer is then baked and fully cured (c) A 200 μm SU8 layer is spun on the substrate. (d) The fluidic outlet channel is defined on the 200 μm SU8 layer using photo-lithography. (e) A drop of UV curable adhesive is placed at the tip of the fiber to create a taper at the entrance of the fiber channel for easier fiber insertion into the PDMS chip.

Photo-transfection of human embryonic kidney (HEK-293) cells

HEK-293 cells, maintained in minimum essential medium (MEM), 1% penicillin-streptomycin supplemented with 10% fetal bovine serum (FBS) (complete medium) were grown in T25 vented top culture flasks and sub-cultured twice weekly at a ratio 1:4. The cells were incubated at 37°C, 5% carbon dioxide and 85% humidity (optimum growth conditions).

Before photo-transfection, approximately 10^4 of cells in 2ml of complete medium were seeded in 35mm diameter type zero glass bottomed Petri dishes. These were incubated to sub-confluency over 24 hours under optimum growth conditions. Following incubation, the monolayer was washed twice with 2ml of OptiMEM each time, to remove the serum. Thereafter the cells were submerged in 60 μ l of serum-free MEM containing 10 μ g/ml of pDsRed2-Mito plasmid deoxyribonucleic acid (pDNA). Targeted photo-transfection of individual cells was then performed with a femtosecond (fs) pulsed Ti:sapphire laser at central wavelength of 790nm, pulse duration 200fs, pulse repetition frequency of 80MHz, 1.1 diameter focal spot with 60mW optical power and an exposure time of 40ms. Following laser irradiation, the DNA-containing medium was aspirated and the monolayer washed once with OptiMEM. 2 ml of the complete medium was then added and the cells incubated under optimum growth conditions for 48 hours before live cell fluorescence imaging.

Incubation of HEK-293 cells with microspheres

Before their incubation with microspheres, the cells were grown at 37°C with 5% CO₂ and 85% humidity (optimum growth conditions). The experimental procedure for incubating the adherent HEK-293 cells with the 2 μ m polymer spheres involved seeding approximately 10^5 cells in 2ml complete medium onto sterile 30mm diameter culture plates prior to microsphere treatment. These cells were grown to sub-confluency overnight within optimum growth conditions. The following day (~ 24 hours post plating), 2ml of culture supernatant that was left on top of the samples was aspirated and replaced with the same volume of media containing 2 μ m diameter spheres. We use hard-dyed (internally dyed) red fluorescing polymer microspheres (Duke Scientific) which have the dye incorporated throughout the polymer matrix (and so are not easily quenched) with a 2 μ m diameter. The microspheres were made of polystyrene with a density of 1.05g/cm³ and a refractive index of 1.59. We used this type of fluorescent microsphere as they emit a bright distinctive red color with an improved contrast and visibility relative to the background material thus providing easy detection. These spheres had an excitation maximum at 542nm and an emission maximum of 612nm. Their original stock concentration was 2.3x10⁹ spheres/ml (solid 1%). For experimental purposes, these were then further diluted 1:1000 in the complete growth media depending on the cell line being investigated. After 24 hours of incubation, when the cell line shows maximum internalization of 2 μ m spheres [20], the sample is used for experiments.

Acknowledgments

We thank the UK Engineering and Physical Sciences Research Council for funding. KD is a Royal Society-Wolfson Merit Award Holder.